

Ultraviolet Molecular Emission from T Tauri Stars: H₂, CO, and the Ly α Radiation Field

Kevin France (University of Colorado), Eric Schindhelm (SwRI),
Gregory J. Herczeg (KIAA, Peking University) and the DAO of Tau Team

Abstract –

The composition and spatial distribution of molecular gas in the inner few AU of young (< 10 Myr) circumstellar disks are important components to our understanding of the formation and evolution of planetary systems. We present results from a far-ultraviolet (far-UV) spectroscopic survey of H₂ and CO emission in protoplanetary disks. Using the new and refurbished spectrographs onboard the Hubble Space Telescope, we observe tens to hundreds of photo-excited molecular emission lines in every gas-rich disk spectrum, independent of the evolutionary state of the dust disk. All transitional disks in our sample display prominent H₂ emission lines arising from a remnant, inner gas disk. Molecular line-widths and excitation temperatures suggest that the emitting H₂ is concentrated between ~ 0.1 – 3 AU, while the CO fluorescence originates between 2 – 10 AU. The UV H₂ emission appears to trace similar disk radii as M-band CO measurements, but the UV- and IR-emitting CO populations appear to be spatially separate. We use these data to reconstruct the local Lyman-alpha radiation field, finding that Lyman-alpha dominates the far-UV energy budget in all cases.

Observations –

The data were obtained as part of HST programs 11533, 12036 (PI – J. Green), 11616 (PI – G. Herczeg), and 11828 and 12361 (PI – A. Brown). The targets were observed with the COS G130M and G160M modes, and STIS E140M. The COS spectra cover $1140 \leq \lambda \leq 1760 \text{ \AA}$ at $R = 18,000$, the STIS spectra cover $1150 \leq \lambda \leq 1690 \text{ \AA}$ at $R \approx 45,000$.

The spectra shown below are typical of the CTTS sample and are spectrally resolved. Kinematic broadening dominates the observed H₂ line profiles.

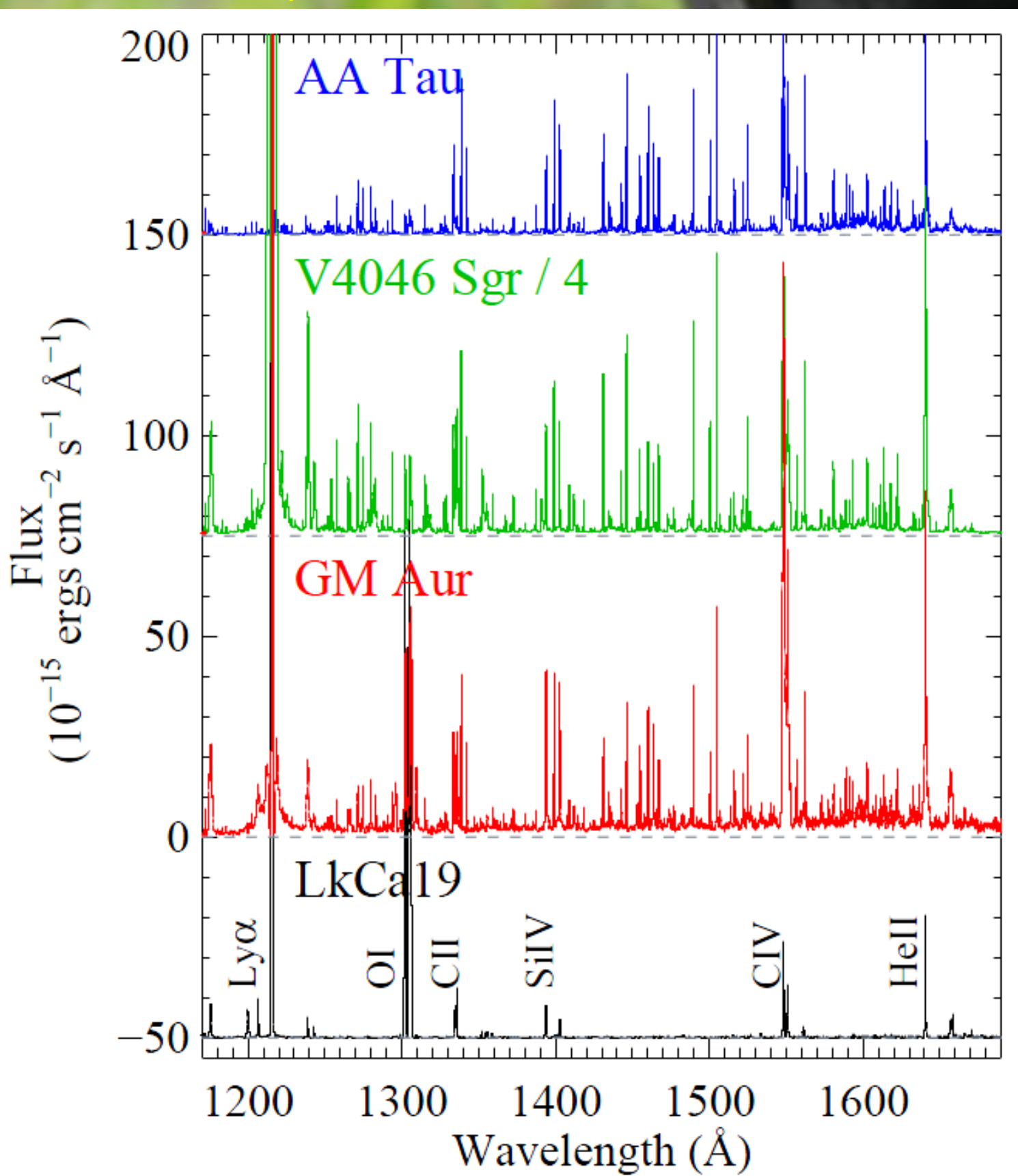
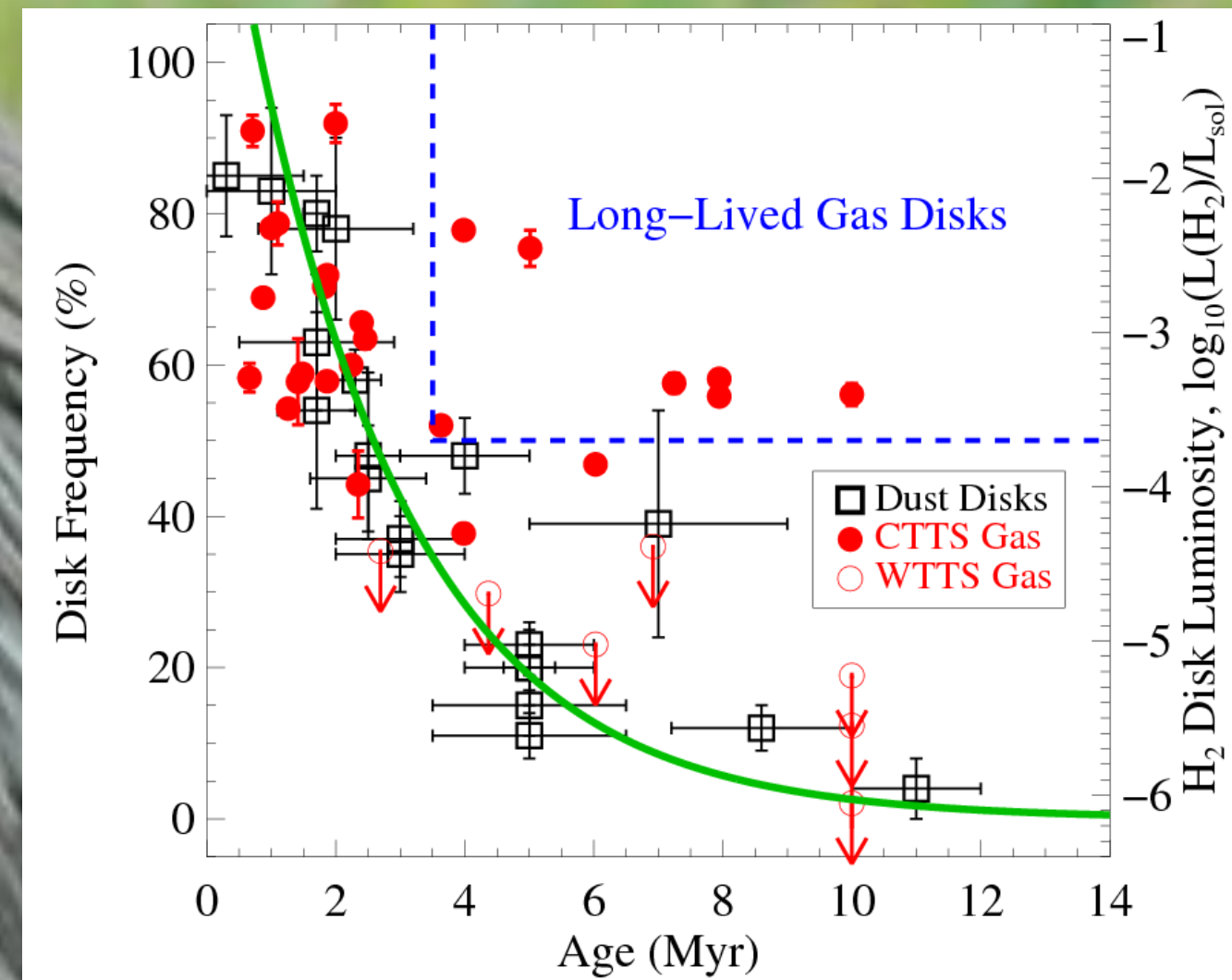


Fig 1 – Above: Example COS G130M + G160M observations of primordial \rightarrow WTTS disk systems. Except for the atomic lines identified in the spectrum of LkCa 19, most of the emission lines in the spectra of the other three stars are fluorescent H₂ and CO emission lines pumped by Ly α . **Left:** Resolved H₂ velocity profiles provide information on the spatial distribution of the gas. The COS LSF is shown as the dash-dotted line. **Below:** Complete COS spectrum of V4046 Sgr with relevant lines marked.

H₂ –

We observe fluorescent H₂ emission, excited by Ly α photons, in 100% of the accreting sources, including all of the transitional disks in our sample (CS Cha, DM Tau, GM Aur, UX Tau A, LkCa 15, HD 135344B, and TW Hya). The spatial distribution of the emitting gas is inferred from spectrally resolved H₂ line profiles. For the disk-dominated targets, the H₂ emission originates predominantly at $r < \sim 3$ AU. Spectral synthesis modeling finds $T(\text{H}_2) \sim 2500 \pm 1000$ K and $\log_{10}(N(\text{H}_2)) \sim 19 \pm 1$. H₂ gas disks are observed to persist to at least 10 Myr, although more data are needed to characterize the H₂ disk lifetime.



CO –

We observe CO A-X band emission in ~60% of our CTTS sources. This CO is excited by UV line photons, predominantly H I Ly α . The CO emission displays rotational structure that reflects the temperature of the CO-bearing gas and the shape of the exciting Ly α radiation field. Spectral synthesis modeling finds CO parameters in the range: $N(\text{CO}) \sim 10^{18-10^{19}} \text{ cm}^{-2}$, $T_{\text{rot}}(\text{CO}) \sim 300 \pm 200$ K for the Ly α -pumped emission.

We also identify the CO A-X (0-1), 11597 and (0-3), 11712 bands in several systems. See poster 2B024 (author: Matt McKinjin) for details of CO absorption line spectroscopy through CTTS disks.

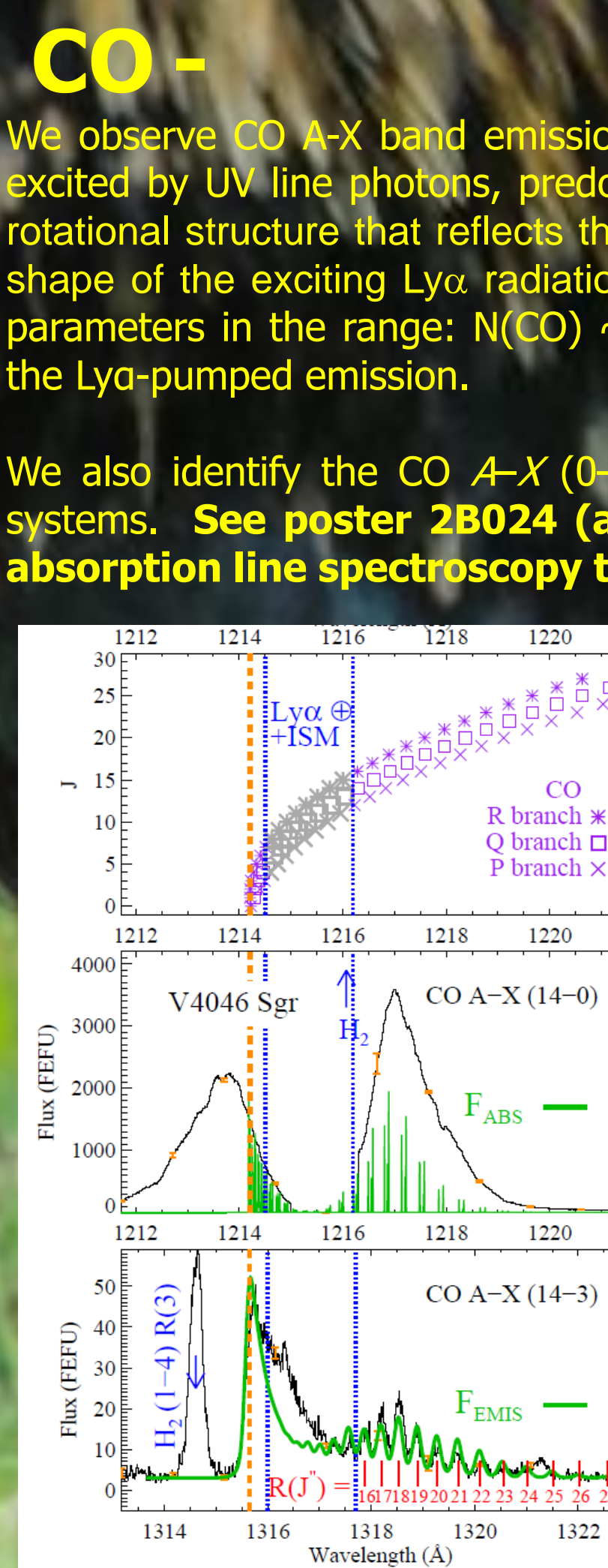


Fig 3 – Above: Graphical description of the H I Ly α pumping line in V4046 Sgr: the observed V4046 Sgr Ly α emission line and the (14-3) CO emission band. The green curves show our model. **Right:** (14-3) and (14-4) fluorescent band emission from some of the targets presented by Schindhelm et al. (2012a). OI] contaminates some (14-4) bands.

Fig 2 – Above: Far-UV H₂ emission lines are a sensitive measure of the molecular disk surface. Dust disk dissipation has a characteristic timescale of 2 – 4 Myr (open squares, adapted from Wyatt 2008), while a number of gas-rich disks are observed to persist to ~ 4 – 10 Myr (filled red circles; France et al. 2012b)

Left: 1430–1470 Å spectral region for the gas-rich targets plotted in Figure 1. All of the strong spectral features in this bandpass are emission lines from Ly α -pumped fluorescent H₂. Objects are plotted in order of decreasing near-IR dust excesses: AA Tau (primordial, $\tau_{1.3-3} = -0.51$), V4046 Sgr (pre-transitional), has a sub-AU scale hole in the inner disk dust distribution, and GM Aur (transitional, $\tau_{1.3-3} = 1.75$) has an ~24AU hole in the inner dust disk (Calvet et al. 2005).

Ly α and the 912 – 1700 Å Radiation Field –

Due to resonant scattering of neutral hydrogen in the interstellar and circumstellar media, the intrinsic Ly α radiation field cannot be directly measured. We utilize the technique of Ly α emission profile reconstruction using the fluorescent H₂ lines as a tracer of the Ly α radiation field incident on the disk surface. This method uses the measured H₂ emission line strengths for a given $[v, J'] \rightarrow [v'', J'']$ progression to determine the total absorbed Ly α flux at a given pumping wavelength. The grid of Ly α fluxes is then fit with an intrinsic line shape and intervening absorber to infer the local Ly α profile and reproduce the observed emission line shape. We have also created new FUV continuum spectra for 16 targets. We identified 210 unique spectral points where a 0.75 Å (approximately 10 spectral resolution elements) emission line-free window can be found between 1138 and 1791 Å. Combining these with the molecule-subtracted observed hot gas line profiles, we can determine the full FUV energy budget from CTTSs. Ly α dominates the FUV radiation output with an average fractional luminosity of 88.1 ± 7.3 %. The FUV continuum is the second largest energy source, with 8.4 ± 5.2 %. The contribution from the C IV 1548,1550 Å doublet is 2.1 ± 1.6 %, and the remaining hot gas emission lines make up < 5% in all cases (see Table).

Target	$F_{\text{Ly}\alpha}^a$ (erg cm ⁻² s ⁻¹)	$\log_{10}(F_{\text{Ly}\alpha}/G_0)^b$	FUV Continuum (%)	Ly α c (%)	C IV (%)	Other ^d (%)
AATAU	3.1×10^4	7.3	2.8	95.9	0.8	0.6
BPTAU	3.5×10^4	7.3	16.8	75.7	4.5	3.1
DETAU	1.5×10^5	7.0	9.2	88.0	2.0	0.9
DFTAU	2.3×10^5	8.2	2.1	97.2	0.4	0.2
DMTAU	4.3×10^5	6.4	8.4	88.0	1.7	1.9
DHTAU	4.0×10^4	7.4	46.2	49.4	3.3	1.0
GM AUR	1.2×10^5	6.9	9.9	86.2	2.4	1.5
HNTAU	1.2×10^5	6.9	10.1	88.4	0.9	0.5
LKCA15	1.6×10^5	7.0	6.5	90.4	2.1	1.0
RECX11	2.3×10^5	6.2	4.6	90.9	2.9	1.7
RECX15	4.8×10^5	6.5	2.8	96.7	0.3	0.3
RULUPI	2.8×10^5	7.2	17.6	79.8	2.0	0.7
SUAUR	3.3×10^5	7.3	8.4	88.3	2.1	1.2
TW HYA	9.7×10^5	6.8	16.7	71.9	6.5	4.9
UXTAU	5.6×10^5	6.5	4.8	92.2	1.7	1.3
V4046SGR	1.5×10^6	7.0	5.3	91.8	1.2	1.8
Average ^e	7.0 ± 0.5	7.0 ± 0.5	8.4 ± 5.2	88.1 ± 7.3	2.1 ± 1.6	1.4 ± 1.2

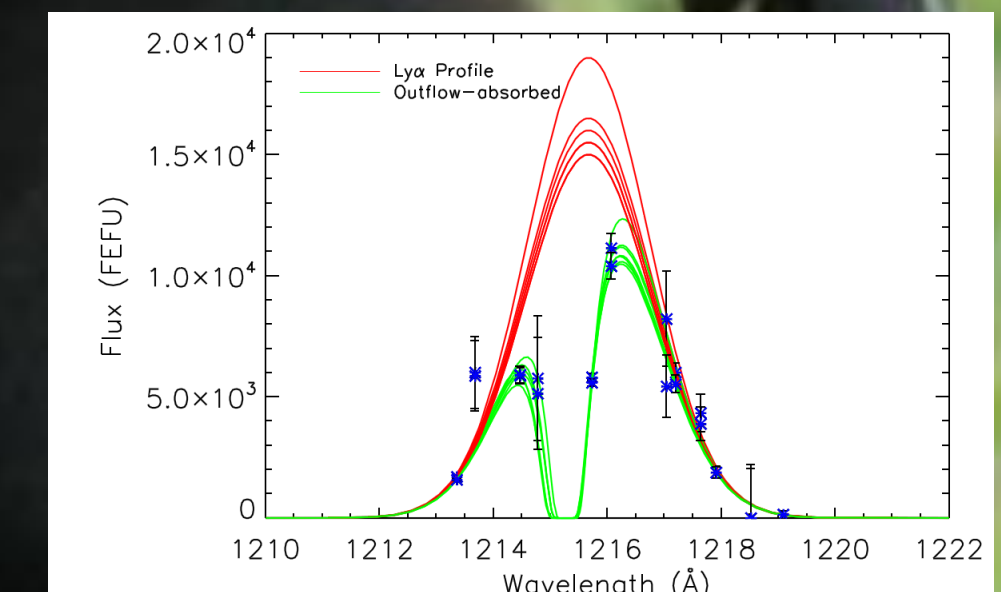


Fig 4 – Left: The table shows the relative contribution of each component to the total FUV irradiance for a sample of 16 high-resolution (912-1700Å) radiation fields assembled by France et al. 2013 (in prep.; http://cos.colorado.edu/~kevinf/ctts_fuvfield.html) **Above:** We use the photoexcited H₂ lines to reconstruct model Ly α profiles. Each pair of intrinsic (red) and outflow-absorbed (green) profiles are a best fit to a different set of $[M(\text{H}_2), T(\text{H}_2)]$ -based incident fluxes (blue asterisks).

H₂ and CO Emission Radii –

Figure 5 compares the Gaussian FWHMs of H₂ and 4.7 μm fundamental band CO emission (IR-CO) for the subsample of our targets that have been observed by the NIRSPEC instrument on Keck II and Phoenix on Gemini South (Salyk et al. 2011). At right, we show the linewidths of photo-excited H₂ and CO (UV-CO; France et al. 2011; Schindhelm et al. 2012). The linewidths of UV-CO are systematically narrower than those of UV-H₂, suggesting a scenario where the UV-CO originates in a cooler molecular layer ($T_{\text{rot}}(\text{CO}) \sim 500$ K) at larger semi-major axes ($a \geq 2$ AU) than both the UV-H₂ and the IR-CO.

The emerging picture of the UV molecular emission environment is shown on the cartoon below.

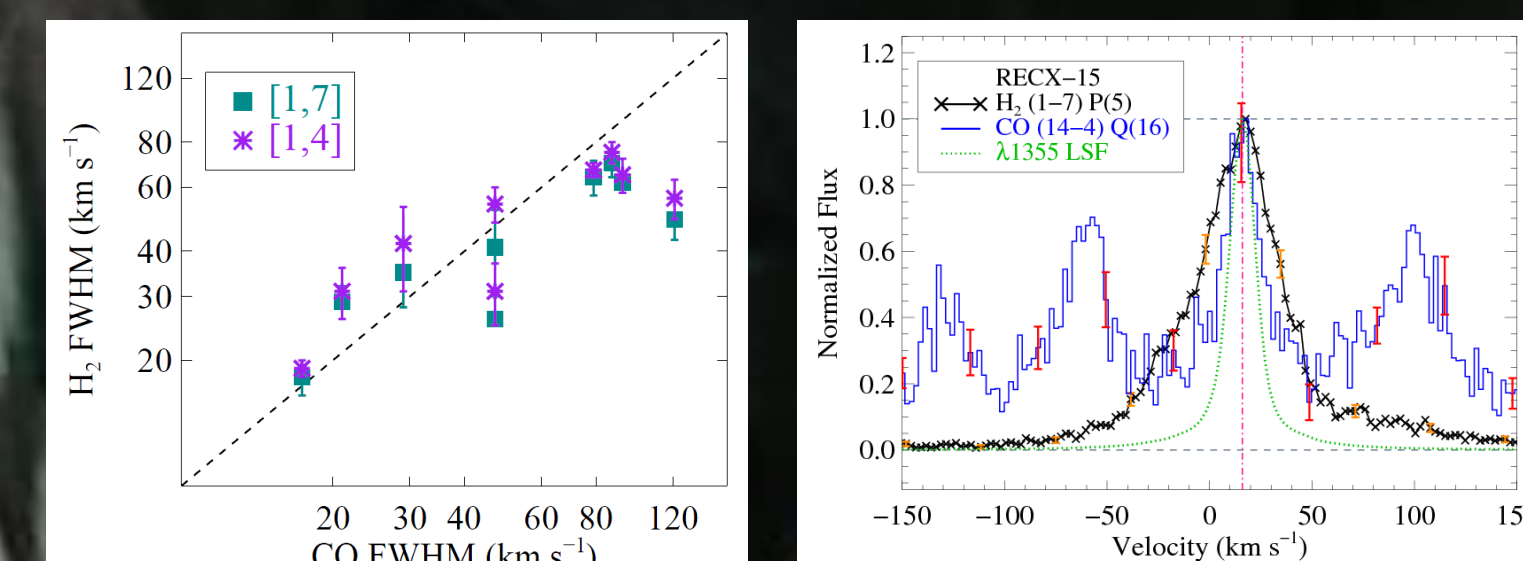
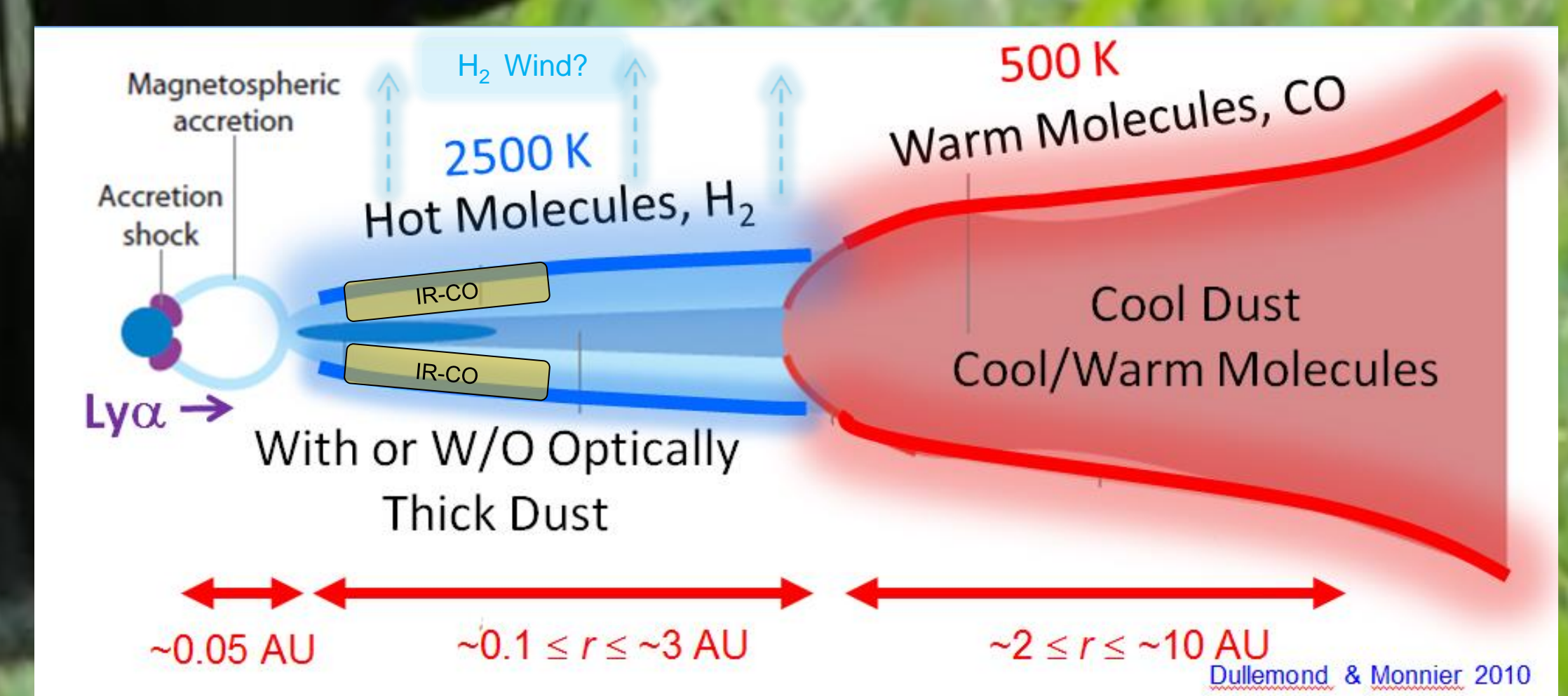


Fig 5 – Left: Comparison of the Gaussian FWHMs of the fluorescent H₂ and the CO fundamental emission. **Right:** Comparison of line shapes for fluorescent H₂ and fluorescent CO emission in the CTTS RECX-15 (ET Cha). **Below:** Schematic representation of the UV molecular emitting regions.



Acknowledgments-

We thank the DAO of Tau team (in particular, Alex Brown) for enjoyable discussions during the course of this work. This work was supported by NASA grant NNX08AC146 to the University of Colorado at Boulder (HST programs 11533 and 12036) and made use of data from HST GO programs 11828, 12361, 8041, and 11616.

For More Information:
kevin.france@colorado.edu
<http://cos.colorado.edu/~kevinf/>

